ARTICLE

Comparison of microbial and transient expression (tobacco plants and plant-cell packs) for the production and purification of the anticancer mistletoe lectin viscumin

Benjamin B. Gengenbach[1,2]* | Linda L. Keil[2]* | Patrick Opdensteinen[1,2] | Catherine R. Müschen[1,2] | Georg Melmer[3] | Hans Lentzen[4] | Jens Bührmann[3] | Johannes F. Buyel[1,2]

[1]Integrated Production Platforms, Fraunhofer Institute for Molecular Biology and Applied Ecology IME, Aachen, Germany

[2]Institute for Molecular Biotechnology, RWTH Aachen University, Aachen, Germany

[3]Pharmedartis GmbH, Aachen, Germany

[4]MELEMA Pharma GmbH, Hamburg, Germany

Correspondence
Johannes Felix Buyel, Fraunhofer Institute for Molecular Biology and Applied Ecology IME, Forckenbeckstraße 6, 52074 Aachen, Germany.
Email: johannes.buyel@rwth-aachen.de

Abstract

Cancer is the leading cause of death in industrialized countries. Cancer therapy often involves monoclonal antibodies or small-molecule drugs, but carbohydrate-binding lectins such as mistletoe (*Viscum album*) viscumin offer a potential alternative treatment strategy. Viscumin is toxic in mammalian cells, ruling them out as an efficient production system, and it forms inclusion bodies in *Escherichia coli* such that purification requires complex and lengthy refolding steps. We therefore investigated the transient expression of viscumin in intact *Nicotiana benthamiana* plants and *Nicotiana tabacum* Bright Yellow 2 plant-cell packs (PCPs), comparing a full-length viscumin gene construct to separate constructs for the A and B chains. As determined by capillary electrophoresis the maximum yield of purified heterodimeric viscumin in *N. benthamiana* was ~7 mg/kg fresh biomass with the full-length construct. The yield was about 50% higher in PCPs but reduced 10-fold when coexpressing A and B chains as individual polypeptides. Using a single-step lactosyl-Sepharose affinity resin, we purified viscumin to ~54%. The absence of refolding steps resulted in estimated cost savings of more than 80% when transient expression in tobacco was compared with *E. coli*. Furthermore, the plant-derived product was ~3-fold more toxic than the bacterially produced counterpart. We conclude that plants offer a suitable alternative for the production of complex biopharmaceutical proteins that are toxic to mammalian cells and that form inclusion bodies in bacteria.

KEYWORDS
cancer therapy, design of experiments, molecular farming, plant-cell pack, recombinant viscumin, transient protein expression

----

1 | INTRODUCTION

Cancer is the collective term for more than 100 different diseases involving abnormal cell proliferation (American Cancer Society, 2015), which can occur spontaneously or due to environmental risk factors such as smoking, carcinogenic chemicals or infectious agents (Cummins & Tangney, 2013). Due to the heterogeneous nature of cancer there is no universal treatment, but four different general approaches are used alone or in combination: surgery, radiotherapy, chemotherapy, and immunotherapy (Sudhakar, 2009). The last two can involve lectins (Jiang et al., 2015), which are plant proteins that bind to carbohydrate structures on the cell surface, inducing immunomodulatory effects or apoptosis (Souza, Carvalho, Ruas, Ricci-Azevedo, & Roque-Barreira, 2013). For example, mistletoe (*Viscum album*) lectin 1 (ML1, viscumin) is a type II ribosome-inactivating protein (RIP; Endo, Tsurugi, & Franz, 1988; Olsnes, Stirpe, Sandvig, & Pihl, 1982) that can be used to treat solid tumors (Zwierzina et al., 2011). Viscumin is a heterodimer (Kourmanova, Soudarkina, Olsnes, & Kozlov, 2004) that is naturally synthesized as a single polypeptide precursor and activated by proteolytically removing a central amino acid linker sequence. The active form of the protein comprises an A chain (former N-terminus) rich in α-helices with N-glycosidase activity (Krauspenhaar et al., 2002) and a glycosylated B chain (former C-terminus) mostly composed of β-sheets (Niwa et al., 2003), which binds to carbohydrates on the cell surface (Walsh, Dodd, & Hautbergue, 2013). There are three intra-chain disulfide bonds in the B chain, and the two chains are covalently linked by a fourth disulfide bond (Olsnes et al., 1982). The toxicity of purified viscumin (intravenous LD_{50} in mice) is 2.4 µg/kg (Olsnes et al., 1982) which is >10-fold more toxic than the structurally-related ricin toxin from castor bean (*Ricinus communis*) seeds (Audi, Belson, Patel, Schier, & Osterloh, 2005).

Due to its toxicity, viscumin cannot be produced in mammalian cells. A nonglycosylated recombinant viscumin purified from *Escherichia coli* inclusion bodies has been tested in Phase I clinical trials (Zwierzina et al., 2011). However, the resolubilization and refolding of proteins from inclusion bodies is laborious and inefficient (Eiberle & Jungbauer, 2010). Furthermore, *N*-linked glycosylation (as carried out in eukaryotic cells but not bacteria) may increase the potency of viscumin. The expression of this lectin in plants may, therefore, help to achieve high yields, straightforward purification and a more potent product.

The use of plants is especially appealing in light of the recent advances in the downstream processing of biopharmaceutical proteins produced in plant systems (Buyel, 2015; Buyel, Twyman, & Fischer, 2015). Plants are also beneficial because they can synthesize complex proteins with authentic posttranslational modifications (e.g., glycosylation, disulfide bond formation), combined with low-cost upstream production (Buyel & Fischer, 2012), inherent process safety based on the inability of human pathogens to replicate in plants (Commandeur, Twyman, & Fischer, 2003), and

the potential for flexible and very-large-scale production (Buyel, Twyman, & Fischer, 2017). The last two aspects are particularly important when comparing plants to mammalian cells because disastrous contamination with human pathogens is unlikely in plants (Bethencourt, 2009; Zimran et al., 2011) and the manufacturing capacity can be rapidly adapted to market demands. Two general types of expression strategies are available for plants, namely expression in transgenic plants or plant cells (Ma et al., 2015), and transient expression by infiltration with *Agrobacterium tumefaciens*, viral vectors or in cell-free systems (Gengenbach, Müschen, & Buyel, 2018). Here we used tobacco (*Nicotiana tabacum*) Bright Yellow 2 (BY-2) plant-cell packs (PCPs) to screen different expression conditions for recombinant viscumin. We then scaled up to transient expression in intact *Nicotiana benthamiana* plants and purified recombinant viscumin from crude plant extracts by affinity chromatography. Fully assembled viscumin was quantified by surface plasmon resonance (SPR) spectroscopy. We compared the performance and economics of the plant-based process to the corresponding process based on *E. coli*.

2 | MATERIALS AND METHODS

2.1 | Expression vectors and bacterial cultures

The coding sequence of the viscumin *ml1p* gene (Kourmanova et al., 2004) from mistletoe (*V. album*; UniProtKB accession number P81446) was synthesized de novo (Thermo Fisher Scientific, Waltham, MA). The codon usage was adapted to *N. benthamiana* (Fath et al., 2011; Raab, Graf, Notka, Schodl, & Wagner, 2010), unwanted endonuclease recognition sites were removed, and the sequence was inserted into the pTRAc expression vector derived from pPAM (GenBank accession number AY027531), generating vector pTRAc-visFL (Figure 1a). Single-chain expression vectors pTRAc-CHSLPH-visAA-S and pTRAc-CHSLPH-visBA-S were also generated (Figure 1b). In all vectors, transcription was controlled by the Cauliflower mosaic virus double enhanced 35SS promoter and 3′-untranslated region (3′-UTR)/polyA signal. The pTRAc-visFL construct also contained the endogenous 5′-UTR, N-terminal signal peptide and internal linker peptide of the ml1p gene. The pTRAc-LPH-visBA-S and pTRAc-LPH-visBA-S constructs contained the murine heavy chain signal peptide from Tobacco mosaic virus-specific mAb24 targeting of the A and B chains to the apoplast. All PCR and cloning materials were used according to the manufacturer's information (New England Biolabs, Ipswich, MA). Plasmids were propagated in *E. coli* cultured in lysogeny broth (5 g/L yeast extract, 10 g/L tryptone, 10 g/L sodium chloride, pH 7.0) supplemented with 100 mg/L ampicillin at 37°C. *A. tumefaciens* strain GV3101:pMP90RK was used for transient expression in *N. benthamiana* leaves and *N. tabacum* BY-2 PCPs. *A. tumefaciens* cells were cultured in liquid peptone agrobacterium medium PAM4 (Houdelet et al., 2017) supplemented with 50 mg/L carbenicillin and 25 mg/L kanamycin at 28°C.
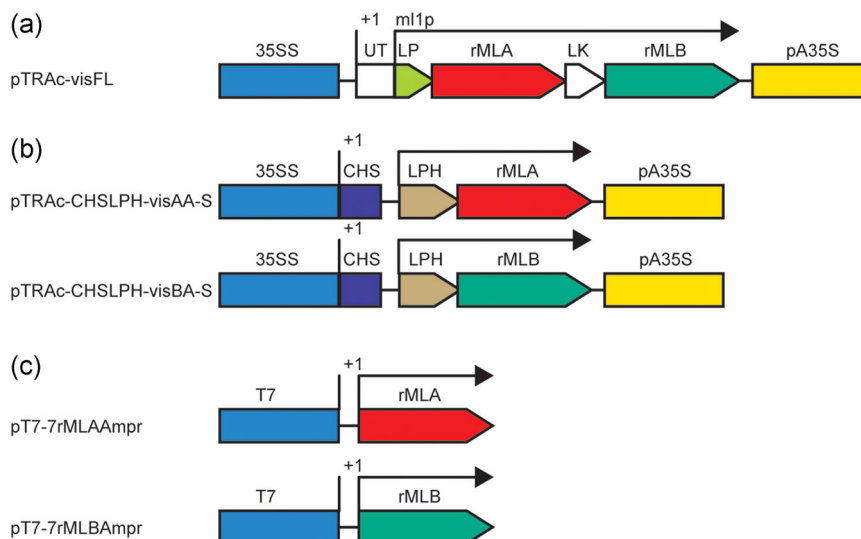
FIGURE 1 Viscumin expression cassettes. (a) pTRAc-visFL (visFL), containing the native full-length viscumin gene including 5′-untranslated region (5′-UTR), and coding sequence (*ml1p*). (b) pTRAc-CHSLPH-visAA-S (visA), encoding the apoplast-targeted viscumin A chain (rMLA), and pTRAc-CHSLPH-visBA-S (visB), encoding the apoplast-targeted viscumin B chain (rMLB). (c) Cassettes for viscumin A chain (7rMLAAmpr) and B chain (rMLBAmpr) expression in *Escherichia coli* . 35SS: Cauliflower mosaic virus double enhanced 35S promoter; UT: Native *Viscum album* 5′-UTR; LP: Native *V. album* signal peptide; LK: Native *V. album* linker peptide; pA35S: Cauliflower mosaic virus 3′-UTR/polyA signal. +1: Transcription start; black arrow: open reading frame. CHS: 5′-UTR of the *Petroselinum hortense* chalcone synthase gene. LPH: murine heavy chain signal peptide from the Tobacco mosaic virus-specific mAb24. T7: Enterobacteria phage T7 promoter. rMLA: viscumin A chain coding sequence. rMLB: viscumin B chain coding sequence [Color figure can be viewed at wileyonlinelibrary.com]

2.2 | *E. coli*-derived viscumin standard

The *E. coli*-derived viscumin, used as reference protein in the course of this study, was produced in house according to a modified protocol based on Eck, Langer, Mockel, Baur, et al. (1999) and Eck, Langer, Mockel, Witthohn, et al. (1999). In brief, two strains of *E. coli* harboring the genetic information for either viscumin A or B chain were cultivated separately in 100-L reactors in defined medium and expression was induced with 0.5 mM IPTG. The cell mass was harvested with a decanter. The cells were resolubilized in 50 mM sodium phosphate (pH 8.0), homogenized in a French-press (GEA, Germany) with 150 MPa and centrifuged at 7,500*g* for 30 min. The pellet was washed three times with four volumes (4 L/kg) of water and centrifuged as before after each wash. The residual protein-pellet was solubilized at 4°C in 50 mM phosphate buffer (pH 6.0) containing 6 M guanidine hydrochloride, 25 mM DTT. The solubilized protein solutions were mixed in a 1.0:1.5 ratio (A:B chain) and refolded for 96 hr.

2.3 | Plant material, infiltration, and expression

N. benthamiana plants were cultivated, infiltrated with *A. tumefaciens* bacterial suspension (OD$_{600 \, nm}$ = 1.0) by manual injection into leaves using infiltration buffer (0.5 g/L Fertilizer MEGA 2 (Planta Düngemittel GmbH, Regenstauf, Germany), 200 μM acetosyringone, pH 5.6) and subsequently incubated as previously described (Buyel, Kaever, Buyel, & Fischer, 2013). The infiltration buffer for PCPs additionally contained 50 g/L sucrose and 2 g/L glucose monohydrate and the OD$_{600 \, nm}$ was

reduced to 0.4. PCPs were cast from 300 μl of continuously cultured BY-2 cell suspension with 20% packed cell volume (200 g wet biomass/L; Holland & Buyel, 2017). A vacuum of 50 kPa was applied for 2 min on a chromabond vacuum manifold (Macherey-Nagel, Düren, Germany) to remove excess medium. The resulting PCPs were in 96-well AcroPrep Advance PP/PE 30–40 μm filter plates (Pall GmbH, Dreieich, Germany) sealed with a gas-permeable membrane with a vapor transmission rate of 4,200 g·m^{-2}·d^{-1} (Macherey-Nagel), covered with a universal microtiter plate plastic lid and incubated at 26°C and 80% relative humidity for up to 7 days.

2.4 | Protein extraction and clarification

N. tabacum BY-2 PCPs (~55 mg) were transferred to 1.5-mL tubes and supplemented with ~0.17 ml extraction buffer (40 mM disodium hydrogen phosphate, 10 mM sodium dihydrogen phosphate, 10 mM sodium metabisulfite), that is 3 ml/g biomass. Buffer conductivity (adjusted with sodium chloride), buffer pH, optional supplementation with detergent Triton X-100, and the number of days of incubation postinfiltration and before extraction were selected using a DoE approach (Table S1) as previously described (Buyel & Fischer, 2013). The design was generated and evaluated using Design Expert v10.0 (Stat-Ease, Minneapolis, MN). PCPs were blended twice in a bead mill (MM 300; Retsch GmbH, Han, Germany) at 28 Hz for 3 min. Extracts were centrifuged at 16,000*g* for 15 min at 4°C and supernatants were used for further analysis. Complete infiltrated *N. benthamiana* leaves were manually removed from plant and extracted as previously described (Buyel et al., 2013). For viscumin purification,

~40 g of infiltrated *N. benthamiana* leaves was homogenized in 3 ml extraction buffer supplemented with 500 mM sodium chloride per g fresh biomass in a Waring blender (Waring; Conair Corp., Stamford, CT) by applying three pulses of 30 s at 30-s intervals. The homogenate was centrifuged at 25,000g for 30 min at 10°C and the supernatant was filtered through 0.2-µm membranes (Minisart; Sartorius-Stedim, Göttingen, Germany) before chromatographic purification.

2.5 | Chromatographic purification of viscumin

Purification was performed on a Janus automated workstation (PerkinElmer, Waltham, MA) using 600-µl RoboColumns packed with lactosyl-Sepharose affinity resin (Repligen GmbH, Weingarten, Germany). We loaded 4 ml of two individual plant extracts onto four columns each at a flow rate of 0.3 ml/min, corresponding to a residence time of 2 min, and eluted three fractions with one column volume per fraction. The base buffer (20 mM sodium dihydrogen phosphate, 1 mM ethylenediaminetetraacetic acid) was supplemented with (a) 300 mM sodium chloride and 0.1 g/L PovidonK17 and adjusted to pH 8.0 for equilibration, (b) 20 mM sodium chloride, 0.1 g/L Tween-80 and adjusted to pH 6.0 for a wash step, or (c) 20 mM sodium chloride, 0.1 g/L Tween-80 and 200 mM lactose monohydrate and adjusted to pH 6.0 for elution.

2.6 | Protein quantitation and immunodetection

The total soluble protein (TSP) concentration was determined using a modified Bradford method (Buyel & Fischer, 2014a). Relative TSP levels were additionally quantified by densitometric analysis of Coomassie Brilliant Blue stained samples (15 µl) after lithium dodecylsulfate–polyacrylamide gel electrophoresis (LDS-PAGE) with NuPAGE 4–12% Bis-Tris gradient gels (Thermo Fisher Scientific) under reducing conditions using AIDA Image Analysis software (Elysia-Raytest GmbH, Straubenhardt, Germany). The A chain of viscumin was detected by LDS-PAGE followed by western blot analysis and densitometric analysis as previously reported (Buyel & Fischer, 2014b). The viscumin A chain-specific mouse mAb TA-5 (Cytavis BioPharma GmbH, Hamburg, Germany) was applied at a concentration of 0.4 µg/ml in PBST (8 mM disodium hydrogen phosphate, 150 mM sodium chloride, 2 mM potassium dihydrogen phosphate, 3 mM potassium chloride, 0.05% [vol/vol] Tween-20, pH 7.4) and incubated overnight at 4°C. First antibody was detected by 1 hr incubation at 22°C with a polyclonal goat antimouse IgG labeled with alkaline phosphatase (1 µg/ml in PBST; Jackson ImmunoResearch, West Grove, PA) followed by colorimetric BCIP/NBT staining according to manufacturer's protocol (Carl Roth GmbH & Co. KG, Karlsruhe, Germany).

Viscumin was quantified by SPR spectroscopy (Howell, Kenmore, Kirkland, & Badley, 1998; Piliarik, Vaisocherova, & Homola, 2009) using a Sierra SPR 4 instrument (Sierra Sensors, Hamburg, Germany). A two-stage assay was performed using a CM5 sensor chip with an EDC/NHS-coupled viscumin B chain-specific 36-2-0 mAb (Cytavis

BioPharma GmbH, Hamburg, Germany). After a wash step, we detected the viscumin A chain specifically with mAb TA-5, thereby quantifying the amount of heterodimeric viscumin molecules. Extract samples were diluted 1:5 in HBS-EP buffer (10 mM hydroxyethyl piperazineethanesulfonic acid, 3 mM ethylenediaminetetraacetic acid, 150 mM sodium chloride, 0.05% [vol/vol] Tween-20, pH 7.4). Two independent bacterial viscumin standard curves of 400, 200, 100, 50, 25, and 0 mg/L were included at the beginning and end of each run. Additionally, a 400 mg/L bacterial viscumin standard was measured after every eight samples to compensate for chip aging. The assay had a coefficient of variance of 1.2% (n = 2) and 2.2% (n = 5) at the lower and upper ends of the standard curve, respectively.

The elution fraction was additionally analyzed by capillary electrophoresis (CE) using a PA 800 plus (Beckman Coulter, Brea, CA). The sample was quantified in two consecutive injections for 20 and 50 s at 5.0 kV against a bacterial viscumin standard curve of 300, 200, 100, 50, 20, 5 and 0 mg/L. Furthermore, elution fraction samples were spiked with 20 mg/L bacterial standard and analyzed as before.

2.7 | De-glycosylation treatment

Purified *N. benthamiana* full length and *E. coli* refolded recombinant viscumin in elution buffer were treated with PNGaseA (New England Biolabs, Ipswich, MA) under denaturing (4.8 ng of viscumin treated at 100°C for 10 min/unit PNGaseA enzyme, 37°C for 1 hr) or native conditions (2.4 ng of viscumin per unit PNGaseA enzyme, 37°C for 24 hr), according to manufacturer's protocol. As a control, native condition samples were inactivated by incubation at 100°C for 20 min following de-glycosylation treatment.

2.8 | Cytotoxicity assay

Viscumin samples were diluted to 0.1 mg/L in cell culture medium (RPMI 1640 + Glutamax with 2% [vol/vol] fetal bovine serum; Thermo Fisher Scientific) and a seven-step 1:4 serial dilution was prepared. From each dilution 20 µl were added to 80 µl of human acute monocytic leukemia cell line THP-1 (Tsuchiya et al., 1980) corresponding to 10^4 cells/well in RPMI 1640 + Glutamax with 10% (vol/vol) fetal bovine serum in a 96-well standard tissue culture plate (Sarstedt, Nuembrecht, Germany), resulting in a final toxin concentration ranging from 0.3 ng/L to 20,000 ng/L. Zeocin (1.0 mg; Thermo Fisher Scientific) or de-glycosylation buffer (1.75 µl) were added as positive and negative controls, respectively, to 100 µl of cells (n = 3).

Following incubation for 48 hr at 37°C and 5.0% (vol/vol) carbon dioxide, 50 µl of 2,3-bis(2-methoxy-4-nitro-5-sulfophenyl)-5-[(phenylamino)carbonyl]-2H-tetrazolium hydroxide (XTT) working reagent (200 µl phenazine ethosulfate (1.67 g/L in water) + 10 ml XTT (1.0 g/L in phosphate-buffered saline), SERVA Electrophoresis GmbH, Heidelberg, Germany) was added

to each well and further incubated for 3 hr. Formazan absorbance was measured at 450 nm against a reference wavelength of 650 nm. Averaged zeocin positive control baseline signal was subtracted from samples and negative controls. Samples were normalized relative to de-glycosylation buffer negative control cell survival.

2.9 | Statistical testing

The α-level was .05 in all cases, first using the Kolmogorov–Smirnov test to ensure normal distribution, then a two-sample f test to confirm equal variances, and third a two-sample two-sided Student's t test to investigate differences between the sample means. Kolmogorov–Smirnov was omitted when the mean and standard deviation (SD) were predicted by Design Expert v10.0 software (StatEase) based on a previously established model.

3 | RESULTS AND DISCUSSION

3.1 | High concentrations of the viscumin A chain are produced using a full-length construct

We transiently expressed full-length viscumin (visFL), using the native 5′-UTR and coding sequence, integrated in construct pTRAc-visFL. We also expressed the individual A chain (visA) using construct pTRAc-CHSLPH-visAA-S, or the A chain together with the separate B chain (visB) using construct pTRAc-CHSLPH-visBA-S in either N. tabacum BY-2 PCPs (Figure 2a) or in the leaves of intact N. benthamiana plants (Figure 2b) by infiltration with A. tumefaciens. Single-chain constructs visA and visB carried a recombinant signal peptide for secretion into the apoplast of intact plants or into the extracellular space of BY-2 suspension cells to circumvent immediate self-intoxication of the respective host. We detected a band of ~30 kDa in all samples by western blot analysis 5 days postinfiltration (dpi) using the A
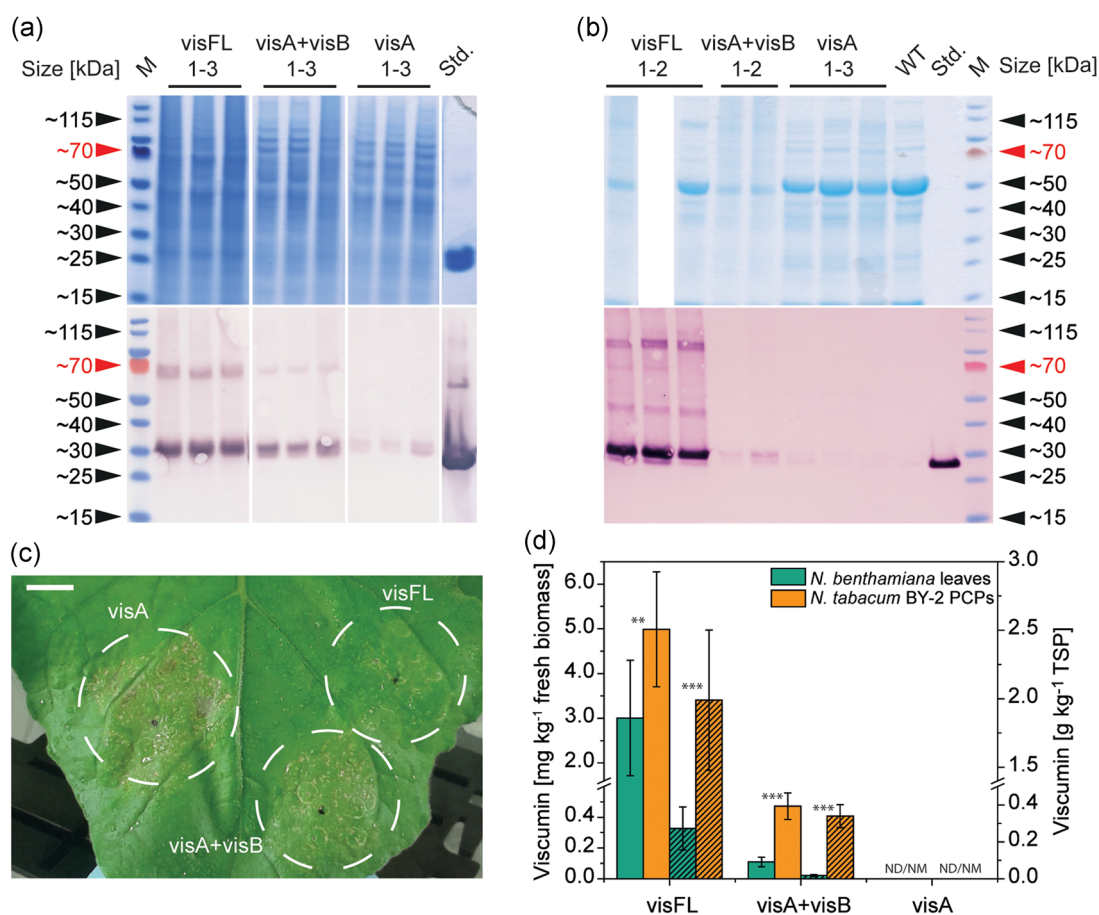

FIGURE 2 Viscumin expression in *Nicotiana tabacum* BY-2 PCPs and *N. benthamiana* leaves at 7 and 5 days postinfiltration (dpi), respectively. (a) Analysis of 15 μl samples derived from *N. tabacum* Bright Yellow 2 (BY-2) plant-cell packs (PCPs) by lithium dodecylsulfate–polyacrylamide gel electrophoresis (LDS-PAGE) followed by staining with Coomassie Brilliant Blue (top) and a western blot using primary monoclonal antibody (mAb) TA-5 and an alkaline phosphatase-labeled goat antimouse IgG secondary antibody. (b) Corresponding analysis of 15 μl samples from *Nicotiana benthamiana* leaves. The LDS-PAGE lane for visFL 3 is missing due to sample loss. M: Marker; 1–3: biological replicates; Std.: 500 ng of viscumin standard (nonglycosylated) purified from *Escherichia coli* . (c) Expression of viscumin in *N. benthamiana* leaves using constructs visA, visA + visB, and visFL. Bar = 10 mm. (d) Viscumin heterodimer yields relative to fresh biomass and TSP-mass at 5 dpi in *N. benthamiana* leaves ($n = 4$) and at 7 dpi in *N. tabacum* BY-2 PCPs ($n = 11$, model based, Tables S1 and S2) determined by surface plasmon resonance spectroscopy. Hatched columns indicate viscumin content per total soluble protein (TSP). Significance of differences between platforms: **$p < .01$, ***$p < .001$ (two-sided Student's t test, $\alpha = .05$) [Color figure can be viewed at wileyonlinelibrary.com]

chain-specific monoclonal antibody (mAb) TA-5. This band migrated slightly slower than the bacterial nonglycosylated viscumin A chain standard (~28 kDa). It corresponded to the anticipated size of the N-glycosylated viscumin A chain (~30 kDa) which includes the mass of the polypeptide plus 1.9 kDa representing a simple N-glycan added to a single predicted acceptor site (Chauhan, Rao, & Raghava, 2013). Such glycosylation was expected due to vacuolar targeting (Strasser, 2014) by means of an internal signal sequence of the pro-toxin (Frigerio et al., 2001). The highest yield of the viscumin A chain, relative to the other infiltration sets, was detected in the visFL samples. In the PCPs and intact leaves, the visFL:visA + visB:visA ratios for the viscumin A chain yield were 6.8:4.0:1.0 and 35:3.5:1.0, respectively. In the visFL and visA + visB PCP samples, we also detected a ~65 kDa band corresponding to the anticipated size of an N-glycosylated viscumin heterodimer or an A chain homodimer, as previously reported in E. coli (Kourmanova et al., 2004). Apart from the gene design (full-length vs. separate chains), the difference in signal peptides and 5′-UTRs may have also affected the A chain yields observed for the three expression setups (Jansing & Buyel, 2018; Meshcheriakova, Saxena, & Lomonossoff, 2014). Low absolute protein concentrations may have prevented dimer detection in the visA samples.

3.2 | Expression of the viscumin A chain alone causes the browning of host cells and tissues

As well as achieving lower product yields (Figure 2a,b), infiltration with visA reduced the TSP content in PCP extracts by ~0.30 g/g compared with visFL (Figure 2a) as determined by densitometric analysis of LDS-PAGE scans. Furthermore, visA alone or in combination with visB caused the N. benthamiana leaves to turn brown (Figure 2c). This probably represents the toxic effect of the free A chain on the host cells, for example, due to cytosolic retro-translocation of the endoplasmic reticulum (ER)-targeted A chain (Agapov et al., 1999; Wesche, Rapak, & Olsnes, 1999). Interestingly, these detrimental effects were substantially reduced when viscumin was expressed using the full-length precursor visFL. We propose two beneficial mechanisms relating to visFL expression. First, expressing the heterodimer can inactivate the toxic subunit as previously shown for viscumin (Agapov et al., 1999; Richardson et al., 1989) and ricin in N. tabacum protoplasts (Frigerio, Vitale, Lord, Ceriotti, & Roberts, 1998), whereas expression of the nontoxic B chain had a scavenging effect on the heterodimer taken up by HeLa cells (Spooner et al., 2004). Second, the linker sequence between the A and B chains can trigger Golgi-mediated transport (Hillmer, Movafeghi, Robinson, & Hinz, 2001) of the glycosylated pro-toxin from the ER to storage vacuoles (Frigerio et al., 2001), where the linker is removed by a vacuolar endoproteinase (Lord, 1985) and the active toxin is safely stored. These beneficial effects of the linker are a common feature of type II RIPs (Fredriksson et al., 2015) and would clearly not be expected when coexpressing the individual chains (visA + visB). Accordingly, we observed a gradient of deleterious effects (browning, low TSP, and low product accumulation) with visA showing the greatest severity, followed by visA + visB and finally visFL. Therefore,

the visFL construct achieved the highest heterodimer yields of 3.0 ± 1.3 mg/kg fresh biomass or 0.00027 ± 0.00011 kg/kg TSP (arithmetic mean [AM] ± SD, n = 9) and 5.0 ± 1.2 mg/kg or 0.00198 ± 0.00051 kg/kg TSP (AM ± SD, n = 11) in N. benthamiana leaves after 5 dpi and in N. tabacum PCPs after 7 dpi, respectively (Figure 2d).

We detected viscumin heterodimer after visA + visB co-infiltration, which indicated that co-transformation took place because dimerization requires disulfide bond formation between A and B chain in the ER (Frigerio et al., 2001). Dimerization can prevent enzymatic degradation and increase product concentrations, as described before for the bacterial toxin AB5 (Kim et al., 2011) and recombinant antibody fragments (Gardner, Aviel, & Argon, 1993). Furthermore, our visA and visB constructs used a nonnative 5′-UTR and signal peptide, which may have contributed to the reduced yields compared with visFL. In contrast, it was shown that expressing the ricin A chain alone in tobacco protoplasts left the product susceptible to proteolytic decay and reduced the yields (Frigerio et al., 1998).

Switching from N. tabacum PCPs to N. benthamiana reduced the heterodimer yield to 70% for visFL but to 30% for visA + visB. The lower yield of A and B chains after co-infiltration into leaves may indicate that more co-transformation events can be achieved using the PCP setup. As a result, more free A chain molecules can potentially contribute to the deleterious effects observed in N. benthamiana leaves compared with PCPs. Additionally, expression levels in N. benthamiana plants might have been lower than in PCPs due to the shorter incubation time of five instead of 7 days, which had to be used to prevent severe necrosis of the leaf tissue at the time of harvest.

3.3 | Transient expression of viscumin in N. tabacum BY-2 PCPs peaks at 7 dpi

Using a design of experiments (DoE, $R^2 = 0.85$, adj. $R^2 = 0.84$, pred. $R^2 = 0.80$, lack of fit not significant) approach we identified 7 dpi as the optimal harvest time in terms of yield, achieving a yield of 5.0 ± 1.2 mg viscumin/kg biomass (1.3 ± 0.3 mg viscumin/L extract). In contrast, pH and conductivity were the only other factors with a significant but much lower effect (Figure 3 and Tables S1 and S2). This was consistent with previous models of recombinant protein expression in N. tabacum plants (Buyel et al., 2013). Adding a detergent had no effect, in contrast to a recent report concerning the extraction of recombinant Phactr1 from PCPs (Gengenbach et al., 2018). We assume that no detergent was required for viscumin because the protein has a defined structure with minimal hydrophobic surface area, in contrast to the intrinsically disordered protein Phactr1 which benefited from detergent-assisted extraction.

3.4 | Viscumin is purified to 0.54 g/g TSP in a single lactosyl-Sepharose affinity chromatography step

We extracted viscumin from N. benthamiana plants infiltrated with visFL. The recovery after clarification by centrifugation and passage through a
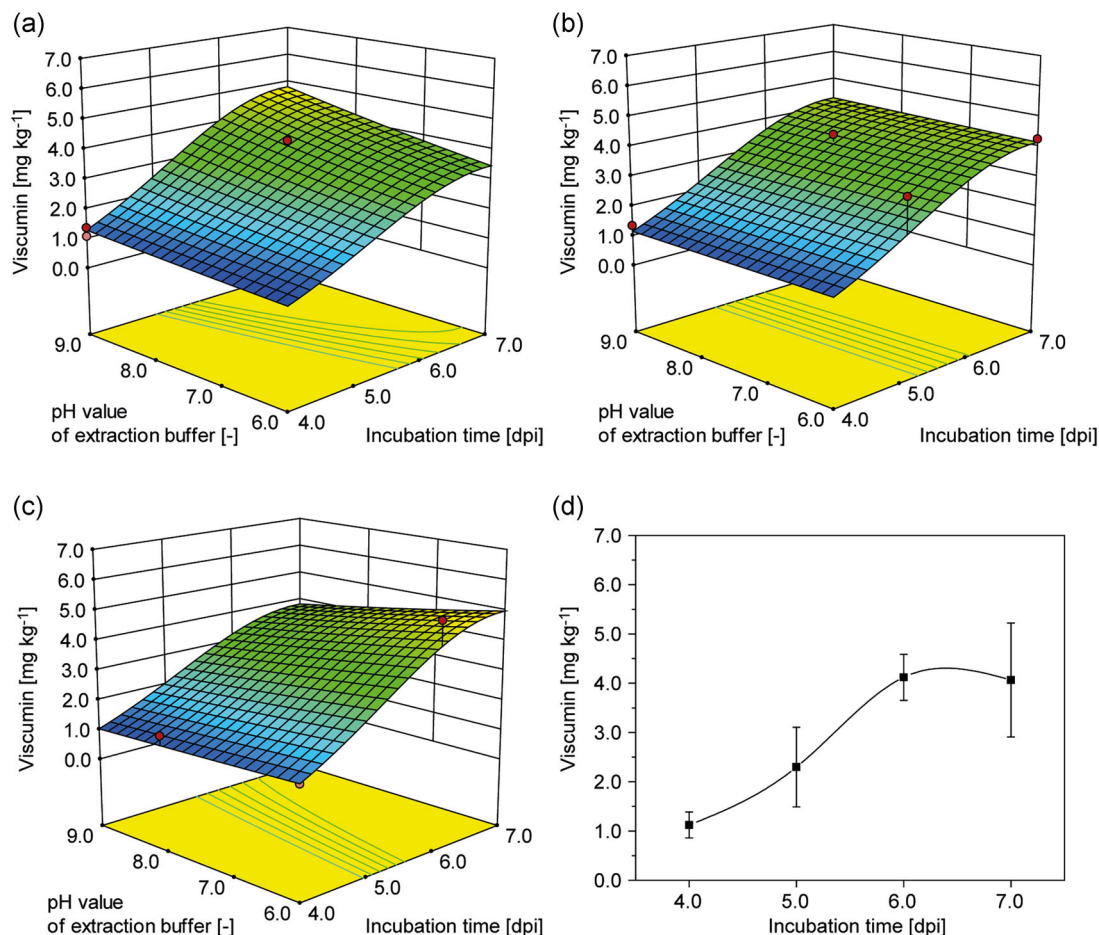
FIGURE 3 Response surfaces representing the viscumin concentration as a function of the extraction buffer pH and conductivity as well as the incubation time following infiltration. Extraction buffer conductivity: (a) 15 mS/cm. (b) 35 mS/cm. (c) 55 mS/cm. (d) Viscumin concentration as a function of incubation time following *Agrobacterium tumefaciens* infiltration averaged over all factor levels (arithmetic mean ± standard deviation, 4 days postinfiltration [dpi] $n = 26$, 5 dpi $n = 12$, 6 dpi $n = 11$, 7 dpi $n = 21$) [Color figure can be viewed at wileyonlinelibrary.com]

0.2-µm filter was 91% (g/g). In a subsequent purification step with a lactosyl-Sepharose affinity resin we concentrated the product 2.0-fold from ~0.51 mg/L in the load to ~1.01 mg/L in the elution buffer, increasing the purity by a factor of ~150 in the process (Table 1). Only minimal amounts of viscumin (in the 0.01–0.02 mg/L range) were detected in the flow-through and wash fractions (Figure 4a). The host cell protein content in the elution fraction was greatly reduced compared with the load fraction (Figure 4b), resulting in a final yield of

1.21 ± 0.34 mg viscumin/kg fresh leaf biomass (AM ± SD, $n = 8$). These results agreed well with previous studies based on other affinity-dependent purification steps, such as immobilized metal-ion affinity chromatography or Protein A affinity chromatography. Such methods achieve more than 100-fold product enrichment in a single step, often resulting in a purity exceeding 0.95 g/g TSP (Buyel, Bautista, Fischer, & Yusibov, 2012; Liu, Ma, Winter, & Bayer, 2010). Even though the host cell protein content in our elution fractions was greatly reduced compared

TABLE 1 Purification and yield of viscumin heterodimer from *Nicotiana benthamiana* leaves

Response	Homogenate (SPR)	Filtrate (SPR)	Elution (SPR)	Elution (CE)
TSP (g/L)	~2.80	~1.00	~0.01	~0.01
Viscumin yield (mg/kg)[a]	2.22 ± 1.53 ($n = 2$)	2.02 ± 0.75 ($n = 8$)	1.21 ± 0.34 ($n = 8$)	7.2 ± 0.1 ($n = 2$)
Purity (g/g)[b]	~0.0002	~0.0005	~0.0681	~0.54
Recovery (g/g)[c]	1.00	~0.91	~0.54	–[d]

Abbreviations: CE, capillary electrophoresis; SPR, surface plasmon resonance; TSP, total soluble protein.
[a]Arithmetic mean ± standard deviation.
[b]Purity as a fraction of TSP in homogenate, filtrate or elution fractions 1 and 2.
[c]Overall viscumin recovery.
[d]A CE-specific recovery cannot be calculated because the method is inadequate to estimate the viscumin concentration in bulk extract.
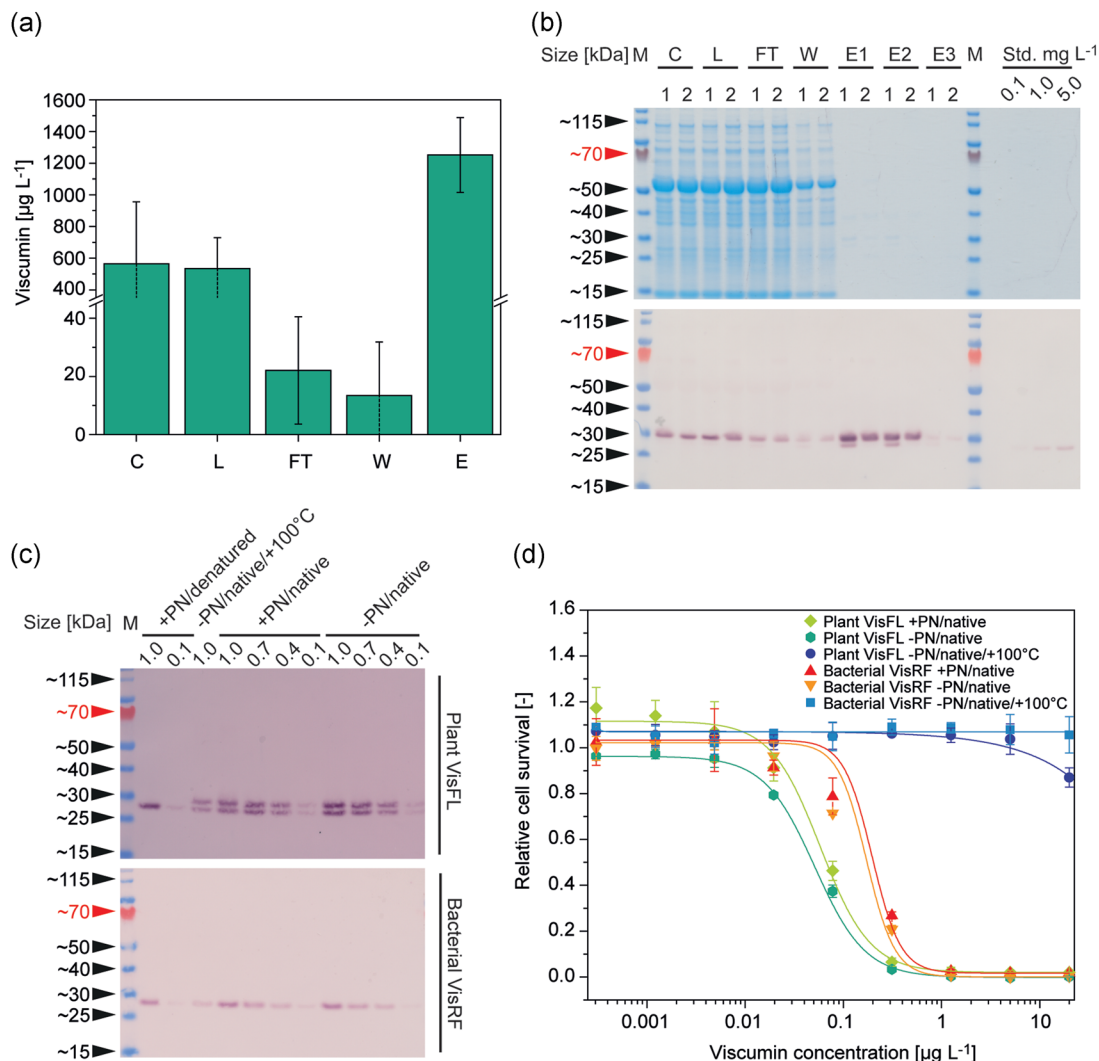
FIGURE 4 Viscumin purity during product purification and final product cytotoxicity. (a) Viscumin concentration determined by surface plasmon resonance spectroscopy (arithmetic mean [AM] ± standard deviation [SD]). (C) centrate (supernatant; $n = 1$, $N = 2$); L, affinity chromatography load ($n = 4$, $N = 8$); FT, flow-through ($n = 4$, $N = 8$); W, wash ($n = 4$, $N = 8$); E, elution fraction 1 ($n = 4$, $N = 8$). (b) Protein composition analysis of 15 µl purification intermediates samples by lithium dodecylsulfate–polyacrylamide gel electrophoresis followed by staining with Coomassie Brilliant Blue (top) and a western blot using primary mAb TA-5 and an alkaline phosphatase-labeled goat antimouse IgG secondary antibody. M: protein size marker; Numbers 1 and 2 in (b) indicate samples from biological replicates; Std.: nonglycosylated viscumin purified from *Escherichia coli*. (c) Western blot analysis of viscumin treated with PNGaseA for de-glycosylation; Plant visFL: full-length viscumin purified from *Nicotiana benthamiana*; Bacterial VisRF: Refolded viscumin (nonglycosylated) purified from *E. coli*; +PN: samples with PNGaseA; −PN: samples without PNGaseA; denatured/native: reaction condition for PNGaseA treatment; +100°C: sample was boiled after PNGaseA treatment; 0.1–1.0: sample dilution factor. (d) 2,3-bis(2-methoxy-4-nitro-5-sulfophenyl)-5-[(phenylamino)carbonyl]-hydroxide (XTT)-cytotoxicity assay of PNGaseA-treated plant VisFL and bacterial VisRF in human cell line THP-1 visualized as cell survival relative to a zeocin positive control (no survival) and 1.75 µl de-glycosylation buffer negative control (full survival; AM ± SD, $n = 3$) [Color figure can be viewed at wileyonlinelibrary.com]

with the load fraction (Figure 4b), the recovery and purity were only 0.6 and 0.08 g/g TSP, respectively (Table 1) in our case as determined by SPR.

We assume that free B chain molecules reduced the product purity because they can bind to the lactosyl-Sepharose resin and thus co-purify with the full-length product. Indeed, by means of silver staining we detected a nonhost cell protein of the size of the B chain (~33 kDa) in our elution fractions, which was more abundant than the A chain. Also the nonglycosylated bacterial standard showed an additional band of ~30 kDa, which was not detected by A-chain-specific western blot analysis and corresponded to the size of the B chain (Figures S1a and

S1b). These results were confirmed by SPR where we observed an A:B chain ratio of 1.00:2.14 for the plant-derived viscumin compared with a 1.00:1.10 ratio for the bacterium-derived standard (0.96 mol/mol heterodimer). We further verified these results by subjecting the elution fraction to CE. The plant-derived viscumin showed a retention time of 21.06 min, which was close to the bacterial counterpart for which we measured 21.075 min (Figure S1c). However, when we used the CE result to calculate the product yield we found 6.1 ± 0.1 mg/L of viscumin heterodimer in the elution fraction corresponding to 7.2 ± 0.1 mg/kg fresh leaf biomass (AM ± SD, $n = 2$) and a purity of 0.54 g/g TSP (Table 1).

We concluded that the direct CE-derived yield and purity seemed more likely than the ~1.2 mg/kg and 0.08 g/g, respectively determined by the indirect SPR assay (Figure S2), because the latter can be affected by differential glycosylation patterns of proteins (Uray, Mizuno, Inazu, Goto, & Hudecz, 2014). For example, epitope recognition and binding kinetics of mAbs can differ for glycosylated and nonglycosylated products. This is relevant because (a) the plant-derived viscumin was glycosylated (see next section) whereas the bacterium-derived counterpart, which we used as a standard for SPR, was not and (b) mAbs TA-5 and 36-2-0 used for A and B chain detection during SPR were raised against the nonglycosylated bacterial standard and thus may exhibit differential binding to a glycosylated form of viscumin.

Despite the use of a lectin specific affinity chromatography we also identified a band at ~53 kDa as a host cell protein, most likely ribulose-1,5-bisphosphate carboxylase oxygenase large subunit by means of western blot (Figure S1b). A distinct band of ~26 kDa (Figure S1a) was not detected by a host cell protein-specific polyclonal antibody cocktail (Arfi, Hellwig, Drossard, Fischer, & Buyel, 2016) or A-chain-specific antibody TA-5. We concluded that this impurity was likely a viscumin degradation product. Furthermore, we speculate that both impurities will be easy to remove from the product by size-based purification steps such as ultrafiltration/diafiltration (UF/DF) or size-exclusion chromatography as has been discussed before (Buyel, Twyman, et al., 2015; Lightfoot, Root, & O'Dell, 2008).

3.5 | Plant-derived recombinant viscumin is glycosylated and threefold more toxic than viscumin purified from *E. coli*

The presence of *N*-glycosylation was tested for *N. benthamiana* derived viscumin by PNGaseA treatment and subsequent western blot analysis. Untreated VisFL showed bands at ~30 and ~28 kDa, characteristic for the glycosylated and nonglycosylated A chain monomer (Figures 4c and S1b). De-glycosylation of VisFL samples under denaturing conditions resulted in the disappearance of the ~30 kDa A chain monomer band, and only the 28 kDa band of the plant-derived viscumin remained which matched the size observed for the bacterium-derived standard (Bacterial VisFL; Figure 4c). This ruled out an incomplete processing of the signal peptide as a cause for the two A chain bands. Under non-denaturing conditions, no de-glycosylation of plant VisFL samples was observed and VisFL samples with and without PNGaseA treatment showed the same cytotoxicity (Figure 4d). This can be due to steric hindrance of PNGaseA, for example, due to the native protein folding as observed before (Merry & Astrautsova, 2003). Therefore, it is currently not possible to investigate the effect of viscumin glycosylation on toxicity in more detail without either altering the viscumin amino acid sequence (which may also affect the toxicity) to remove the glycosylation site or to knock-out the responsible glycosyltransferases (which may affect the entire plant) to avoid the glycosylation.

A subsequent cytotoxicity test using human cell line THP-1 showed an ~3-fold increased toxicity of the *N. benthamiana* derived viscumin compared with the *E. coli*-derived microbial standard for both the PNGaseA-treated and untreated samples (Figure 4d). Heat inactivation

of plant and bacterial viscumin samples at 100°C removed their toxic effects. The increased toxicity was observed for glycosylated and PNGaseA-treated native plant-derived viscumin. The latter sample likely still contained glycosylated A chain because the PNGaseA seemed only active under denaturing conditions. However, such conditions would remove viscumin cytotoxicity. Still, our observations were in good agreement with recent publications indicating that a lack of authentic glycan structures can impede the highly specific internalization and trafficking process of type 2 RIPs within the target cell (Taubenschmid et al., 2017). Similar results have been obtained for native viscumin and ricin (a toxin similar to viscumin) where A chain glycosylation increased the toxicity for MOLT-4 leukemia T-cells and HeLa cells 1.5-fold and ~3-fold, respectively, compared with *E. coli*-derived counterparts (Eck, Langer, Mockel, Witthohn, et al., 1999; Simpson, Roberts, & Lord, 1996).

3.6 | The expression of viscumin in plants is beneficial in terms of production process design

Although viscumin has been produced in *E. coli* allowing it to be tested in clinical trials (Zwierzina et al., 2011), the process is complex and difficult to scale up, for example, due to the need for a refolding step in dilute buffers (Eck, Langer, Mockel, Witthohn, et al., 1999). The A and B chains were produced by two different bacterial strains in separate fermentations and both polypeptides formed inclusion bodies. Therefore, laborious resolubilization and refolding steps were necessary in both cases, leading to poor recoveries of 5–10% based on the amount of unfolded polypeptide educts (Eck, Langer, Mockel, Baur, et al., 1999; Eck, Langer, Mockel, Witthohn, et al., 1999), which is typical for such refolding processes (Eiberle & Jungbauer, 2010). Additionally, the product was not glycosylated, which may affect its stability and efficacy (Li et al., 2012). The process developed in *E. coli* required 13 individual steps (Eck, Langer, Mockel, Baur, et al., 1999; Eck, Langer, Mockel, Witthohn, et al., 1999; Figure 5a) which substantially increases both the investment and operational costs for GMP manufacturing, especially if large vessels are required for the refolding step. The complexity also increases the documentation requirements and the likelihood of errors compared with simpler processes. Other plant lectins have been expressed in the yeast *Pichia pastoris* at levels of 6–20 mg/L (Lannoo, Vervecken, Proost, Rouge, & Van Damme, 2007; Oliveira, Felix, Moreira, Teixeira, & Domingues, 2008), which is similar to the ~7 mg/kg that we report here, assuming that 1 kg of plant biomass is approximately equivalent to 1 L of fermentation broth because both contain about 6% (~60 g/kg) dry cell mass (Buyel, Gruchow, Tödter, & Wehner, 2016; Kastilan et al., 2017). However, glycoproteins produced in yeasts often carry predominantly high-mannose rather than complex-type glycans (Strasser, 2016), which increase the risk of an immune response. However, this risk can be reduced if glycoengineered strains are used (Jacobs, Geysens, Vervecken, Contreras, & Callewaert, 2009; Pekarsky et al., 2018; Purcell et al., 2017). Here, this issue was overcome by using plant systems as expression hosts. The yields of ~7 mg/kg we achieved exceed the 1.2 mg/L produced in *E. coli* after refolding. Also, the plant system did not require resolubilization or refolding steps and the
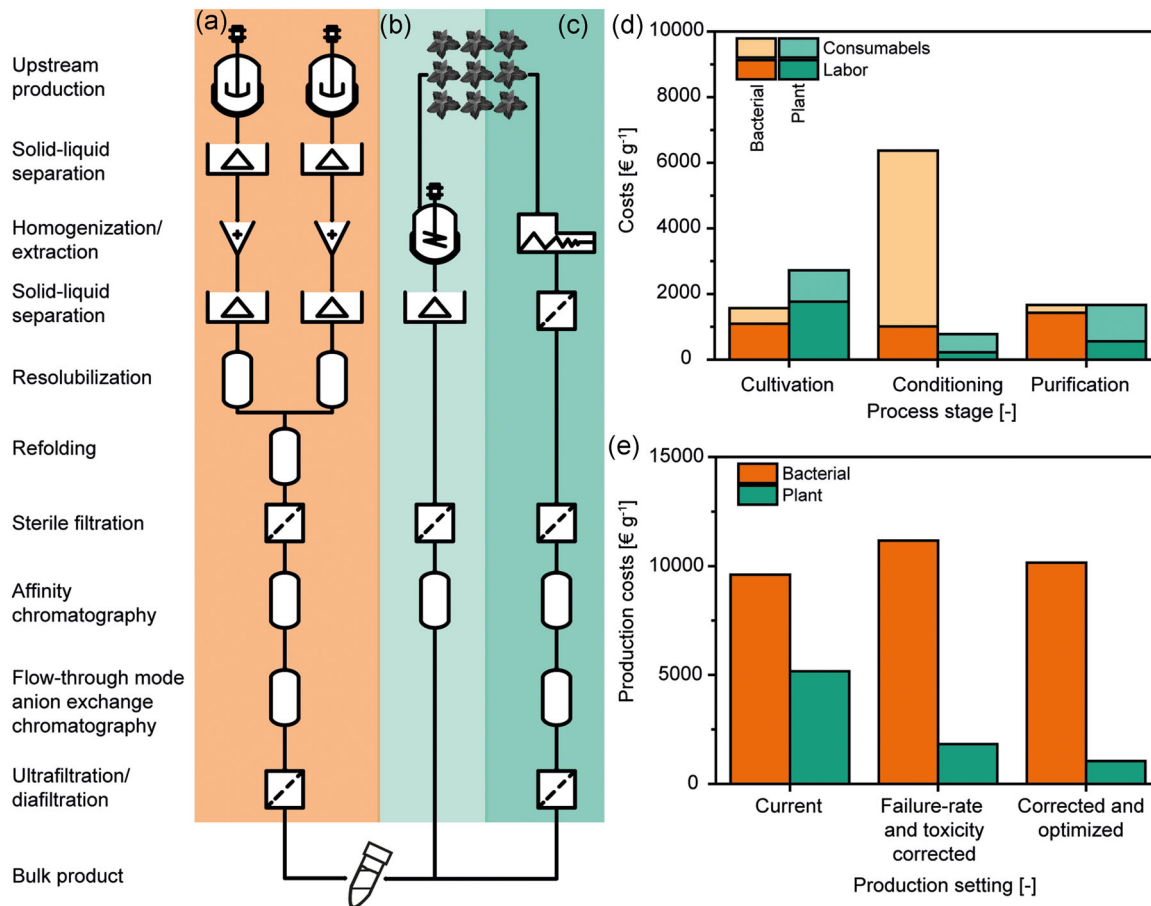
FIGURE 5 Comparison of viscumin production processes. (a) Production in *Escherichia coli* requires separate fermentations and primary processing for the A and B chains and a total of seven downstream steps, four of which need to be carried out twice. (b) The plant-based process we developed consists of only five steps, including plant cultivation, and does not require product resolubilization or refolding. (c) The current plant-based process can be streamlined in the future by replacing semi-continuous extraction and centrifugation with screw-press and pre-coat filtration steps, respectively, as previously suggested (Buyel et al., 2017). (d) Consumables and labor costs associated with the three stages of the bacterial (orange) and plant-based (green) production processes. (e) Production costs per gram of product for the (a) current setting, (b) including a 1% failure rate per process step and toxicity correction and (c) an optimized scenario, for example, using p19 as a gene silencing suppressor for the plant system [Color figure can be viewed at wileyonlinelibrary.com]

viscumin was produced in a single step rather than two separate fermentations, which greatly reduced the process complexity (Figure 5b). Purifying viscumin with a lactosyl-Sepharose affinity resin was less effective in plants than it was in the *E. coli* process. In addition to the higher B chain content, the absence of earlier enrichment steps (which were present in the bacterial process, e.g., separating the inclusion bodies from host cell proteins), may have reduced the purity of viscumin generated using our process. However, even if two additional purification steps such as UF/DF are included in our process, the total number of process steps is still only half as many as required for the *E. coli* process.

3.7 | Isolation of viscumin from a heterologous source achieves higher yields than native mistletoe

In addition to heterologous expression systems, viscumin could potentially be isolated from its natural source, where the product concentration can be several times higher than we achieved

(Olsnes et al., 1982). However, in addition to product concentration, a meaningful comparison of native and recombinant expression systems must consider the cultivation requirements, the useable biomass per plant, for example, by applying a harvest index (Hay, 1995), as well as the space–time yield accounting for typical growth periods and the resulting biomass per unit area.

Mistletoe, the natural source of viscumin, requires up to 20 years to grow in to a bush with a diameter of 1 m (Bussing, 2000). The plant is an obligate parasite, so host plants such as White willow (*Salix alba*) are required (Barney, Hawksworth, & Geils, 1998), and must be maintained and inoculated as well, which substantially increases the cultivation effort and limits the cultivation density, automation potential, containment, and product flexibility. Based on 300,000 White willow trees per km^2 (Lindegaard et al., 2016), seven mistletoe plants per tree, and 8 kg leaf biomass per plant (March & Watson, 2007), up to 840,000 $kg \cdot km^{-1} \cdot year^{-1}$ of leaf biomass could be harvested in forests (Table 2). This would be equivalent to ~57 kg of product per year but would require several years of lead-time to establish a host plantation. In

TABLE 2 Isolation of toxic lectins from native and recombinant hosts

Product (–)	Species (–)	Expression (–)	Organ (–)	Yield (g/kg organ)	Harvest index (–)	Biomass yield (kg·km^{-2}·year^{-1})	Organ yield (kg·km^{-2}·year^{-1})	Toxin productivity (g·km^{-2}·year^{-1})
Viscumin	Nicotiana benthamiana	Recombinant (vertical farm)	Green biomass	0.0072	0.68[a]	91,000,000[b]	61,880,000	445,536
Viscumin	Nicotiana tabacum	Recombinant (open field)	Green biomass	0.0072	0.62	10,000,000[c]	6,200,000	44,640
Viscumin	Viscum album	Native	Green biomass	0.068[d]	n.a.	n.a.	840,000	57,120
Abrin	Abrus precatorius	Native	Seeds	1.7[e]	0.50[f]	630,000[f]	315,000	535,500
Ricin	Ricinus communis	Native	Seeds	3.75[g]	0.10[h]	2,000,000[h]	200,000	750,000

Note: Harvest index: ratio of usable to total fresh biomass.

Abbreviation: CV, coefficient of variance.

[a]CV N. benthamiana 1.2%, N. tabacum 2.8%, n = 3.

[b]Buyel et al. (2017).

[c]Stoger et al. (2002).

[d]Olsnes et al. (1982).

[e]Average concentration of Abrin I–III (Hegde et al., 1991).

[f]Pisum sativum L. used as a best-case estimate for the common Fabaceae family (Lecoeur & Sinclair, 2001).

[g]Simmons and Russell (1985).

[h]Severino et al. (2012).

contrast, tobacco plants can yield up to 10,000,000 kg·km^{-2}·year^{-1} in the open field (Stoger et al., 2002) and N. benthamiana can produce up to 91,000,000 kg·km^{-2}·year^{-1} in vertical farms (Buyel et al., 2017). Even without optimizing expression, for example, by modifying subcellular targeting, the current setup would yield ~8-fold more product than the native host. Furthermore, heterologous expression allows the immediate initiation of production and the direct synthesis of fusion proteins, which is a promising pharmaceutical application for cytotoxins such as viscumin (Buyel, 2018; Weidle, Schneider, Georges, & Brinkmann, 2012). The native host can also contain several isoforms of a RIP. These can differ in their biochemical properties, for example, levels of toxicity, but exhibit similar carbohydrate specificity, which will hinder effective product purification (Hegde, Maiti, & Podder, 1991; Urech, Schaller, & Jaggy, 2006). We therefore conclude that the heterologous production of viscumin is superior to the harvesting of native host plants.

Interestingly, the natural sources of other RIPs such as abrin (Abrus precatorius) and ricin (R. communis) may offer a competitive alternative to heterologous production (Hegde et al., 1991; Simmons & Russell, 1985). The seeds of these plants contain up to 4 g of the target products per kg biomass (Table 2) and R. communis is readily cultivated on an agronomic scale yielding ~200,000 kg·km^{-2}·year^{-1} of seed biomass (Severino et al., 2012). However, they do not show the same pharmacological potential as viscumin.

3.8 | The expression of viscumin in plants has the potential to reduce production costs by ~80%

After the affinity purification step our overall purity was 52% with a yield of 7 mg/kg biomass, whereas the microbial process achieved about 90% purity after the same step and a yield of 42 mg/L. The lower purity we currently observe for the plant-derived product was mostly due to the presence of the free viscumin B chain as discussed above. However, the mass difference between this product-related impurity and the fully assembled viscumin is 35 kDa, corresponding to a factor of >2.0, which should facilitate purification by introducing an UF/DF step as shown for other proteins before (Opdensteinen, Clodt, Müschen, Filiz, & Buyel, 2018). Such a step is unlikely to increase downstream processing costs or to cause additional product losses because an UF/DF step was also required to remove the carbohydrates used during elution from the lactosyl-Sepharose resin in the E. coli process (Figure 5a). Apart from the small-scale process we have described here (Figure 5b), we envisage that a scalable, GMP-compliant process will implement continuous extraction and clarification operations, for example, a screw-press and two filtration stages that we have successfully tested for processing plant biomass (Buyel & Fischer, 2014b; Buyel, Gruchow, & Fischer, 2015), as well as one additional chromatographic purification and a final UF/DF step as in the bacterial process (Figure 5c). Based on these assumptions and a modified cost model reported for plant cultivation (Buyel & Fischer, 2012) as well as our experience with the bacterial process, we compared the manufacturing effort for the two expression platforms. We found that in the current setup using the plant-based process, viscumin production costs were ~5,200€/g, which was about 54% of

-WILEY |

the 9,600€/g we determined for the bacterial process (Figure 5d,e). The bacterial process was dominated by the costs and labor required for the complex refolding process, that was not required in the plant system. When we took a generic 1% failure rate per process step into account and further considered the ~3-fold increased toxicity of the plant-derived product, costs of the plant process dropped to 16% of the bacterial process. Also, the *E. coli* process has been optimized over a period of ~20 years (Eck, Langer, Mockel, Baur, et al., 1999; Eck, Langer, Mockel, Witthohn, et al., 1999), whereas we have not yet optimized the expression of visFL. For example, future processes could incorporate the p19 silencing suppressor and optimized UTRs, which have previously increased the accumulation of other recombinant proteins by 15-fold and 50%, respectively (Garabagi, Gilbert, Loos, McLean, & Hall, 2012; Jansing & Buyel, 2018). We therefore introduced a moderate predicted improvement of 33% for each modification, resulting in a hypothetical increase in expression from 7.2 to 12.0 mg/kg. We also assumed that a 10% yield increase could be achieved in *E. coli* despite the extensive process development that has been carried out already. Using these numbers, we calculated that the cost of goods for the plant-based system could be reduced to ~1,000€/g, which is only ~10% of the cost of the bacterial system. Our estimate of the optimization potential of the plant systems is conservative and according improvements may counterbalance a reduced product yield that can arise by a switch from manual infiltration (used here) to whole plant vacuum infiltration used at large scale. Others have recently reported cost models for the production of recombinant proteins in plants as well, but we did not consider these models here because either the process scale (>60 kg of product; Nandi et al., 2016) or cultivation conditions (greenhouse instead of vertical farm; Walwyn, Huddy, & Rybicki, 2015) did not match the setup in our study.

4 | CONCLUSION

We have expressed full-length viscumin in *N. tabacum* PCPs and *N. benthamiana* leaves at levels of up to 7 mg/kg of purified product. Coexpressing the A and B chains was also possible in both systems but the yield of heterodimeric product was reduced by up to 0.97 g/g, whereas expressing the A chain alone did not produce quantifiable amounts of recombinant protein. The yield of full-length viscumin was comparable with that of plant lectins expressed in yeast but ~6-fold lower than refolded viscumin A and B chains expressed in *E.coli*. However, the bacterial process has a low recovery, requires extensive dilution and is complex, whereas the plant-based process included only half the number of steps. According to a direct cost comparison between the two processes, the plant expression system is currently 50% less expensive, but moderate improvements in yield can reduce production costs by even up to ~88%. In comparison with the native host *V. album*, the heterologous expression approach reduced the lead-time by several years, increased containment as well as space–time yield, and facilitated targeted product modifications. Therefore, producing recombinant viscumin in plants is a useful alternative to both microbial and native systems.

CONFLICT OF INTERESTS

The authors declare that there are no conflict of interests.

ORCID

Johannes F. Buyel http://orcid.org/0000-0003-2361-143X

REFERENCES

Agapov, I. I., Tonevitsky, A. G., Moysenovich, M. M., Maluchenko, N. V., Weyhenmeyer, R., & Kirpichnikov, M. P. (1999). Mistletoe lectin dissociates into catalytic and binding subunits before translocation across the membrane to the cytoplasm. *FEBS Letters*, *452*, 211–214.

American Cancer Society (2015). *Cancer facts and figures 2015*. Atlanta: American Cancer Society.

Arfi, Z. A., Hellwig, S., Drossard, J., Fischer, R., & Buyel, J. F. (2016). Polyclonal antibodies for specific detection of tobacco host cell proteins can be efficiently generated following RuBisCO depletion and the removal of endotoxins. *Biotechnology Journal*, *11*, 507–518.

Audi, J., Belson, M., Patel, M., Schier, J., & Osterloh, J. (2005). Ricin poisoning: A comprehensive review. *Journal of the American Medical Association*, *294*, 2342–2351.

Barney, C. W., Hawksworth, F. G., & Geils, B. W. (1998). Hosts of *Viscum album*. *European Journal of Forest Pathology*, *28*, 187–208.

Bethencourt, V. (2009). Virus stalls Genzyme plant. *Nature Biotechnology*, *27*, 681–681.

Bussing, A. (2000). *Mistletoe: The genus Viscum*. Baco Raton, FL: CRC Press.

Buyel, J. F. (2015). Process development strategies in plant molecular farming. *Current Pharmaceutical Biotechnology*, *16*, 966–982.

Buyel, J. F. (2018). Plants as sources of natural and recombinant anti-cancer agents. *Biotechnology Advances*, *36*, 506–520.

Buyel, J. F., Bautista, J. A., Fischer, R., & Yusibov, V. M. (2012). Extraction, purification and characterization of the plant-produced HPV16 subunit vaccine candidate E7 GGG. *Journal of Chromatography B: Analytical Technologies in the Biomedical and Life Sciences*, *880*, 19–26.

Buyel, J. F., & Fischer, R. (2012). Predictive models for transient protein expression in tobacco (*Nicotiana tabacum* L.) can optimize process time, yield, and downstream costs. *Biotechnology and Bioengineering*, *109*, 2575–2588.

Buyel, J. F., & Fischer, R. (2013). Processing heterogeneous biomass: Overcoming the hurdles in model building. *Bioengineered*, *4*, 21–24.

Buyel, J. F., & Fischer, R. (2014a). Flocculation increases the efficacy of depth filtration during the downstream processing of recombinant pharmaceutical proteins produced in tobacco. *Plant Biotechnology Journal*, *12*, 240–252.

Buyel, J. F., & Fischer, R. (2014b). A juice extractor can simplify the downstream processing of plant-derived biopharmaceutical proteins compared to blade-based homogenizers. *Process Biochemistry, 50,* 859–866.

Buyel, J. F., Gruchow, H. M., & Fischer, R. (2015). Depth filters containing diatomite achieve more efficient particle retention than filters solely containing cellulose fibers. *Frontiers of Plant Science, 6,* 1–11.

Buyel, J. F., Gruchow, H. M., Tödter, N., & Wehner, M. (2016). Determination of the thermal properties of leaves by non-invasive contact free laser probing. *Journal of Biotechnology, 217,* 100–108.

Buyel, J. F., Kaever, T., Buyel, J. J., & Fischer, R. (2013). Predictive models for the accumulation of a fluorescent marker protein in tobacco leaves according to the promoter/5′UTR combination. *Biotechnology and Bioengineering, 110,* 471–482.

Buyel, J. F., Twyman, R. M., & Fischer, R. (2015). Extraction and downstream processing of plant-derived recombinant proteins. *Biotechnology Advances, 33,* 902–913.

Buyel, J. F., Twyman, R. M., & Fischer, R. (2017). Very-large-scale production of antibodies in plants: The biologization of manufacturing. *Biotechnology Advances, 35,* 458–465.

Chauhan, J. S., Rao, A., & Raghava, G. P. (2013). In silico platform for prediction of N-, O- and C-glycosites in eukaryotic protein sequences. *PLOS One, 8,* e67008.

Commandeur, U., Twyman, R. M., & Fischer, R. (2003). The biosafety of molecular farming in plants. *AgBiotechNet, 5,* 1–9.

Cummins, J., & Tangney, M. (2013). Bacteria and tumours: Causative agents or opportunistic inhabitants? *Infect. Agents Cancer, 8,* 1–8.

Eck, J., Langer, M., Mockel, B., Baur, A., Rothe, M., Zinke, H., & Lentzen, H. (1999). Cloning of the mistletoe lectin gene and characterization of the recombinant A-chain. *European Journal of Biochemistry, 264,* 775–784.

Eck, J., Langer, M., Mockel, B., Witthohn, K., Zinke, H., & Lentzen, H. (1999). Characterization of recombinant and plant-derived mistletoe lectin and their B-chains. *European Journal of Biochemistry, 265,* 788–797.

Eiberle, M. K., & Jungbauer, A. (2010). Technical refolding of proteins: Do we have freedom to operate? *Biotechnology Journal, 5,* 547–559.

Endo, Y., Tsurugi, K., & Franz, H. (1988). The site of action of the A-chain of mistletoe lectin I on eukaryotic ribosomes. The RNA N-glycosidase activity of the protein. *FEBS Letters, 231,* 378–380.

Fath, S., Bauer, A. P., Liss, M., Spriestersbach, A., Maertens, B., Hahn, P., … Wagner, R. (2011). Multiparameter RNA and codon optimization: A standardized tool to assess and enhance autologous mammalian gene expression. *PLOS One, 6,* e17596.

Fredriksson, S. A., Artursson, E., Bergstrom, T., Ostin, A., Nilsson, C., & Astot, C. (2015). Identification of RIP-II toxins by affinity enrichment, enzymatic digestion and LC-MS. *Analytical Chemistry, 87,* 967–974.

Frigerio, L., Jolliffe, N. A., Di Cola, A., Felipe, D. H., Paris, N., Neuhaus, J. M., … Roberts, L. M. (2001). The internal propeptide of the ricin precursor carries a sequence-specific determinant for vacuolar sorting. *Plant Physiology, 126,* 167–175.

Frigerio, L., Vitale, A., Lord, J. M., Ceriotti, A., & Roberts, L. M. (1998). Free ricin A chain, proricin, and native toxin have different cellular fates when expressed in tobacco protoplasts. *Journal of Biological Chemistry, 273,* 14194–14199.

Garabagi, F., Gilbert, E., Loos, A., McLean, M. D., & Hall, J. C. (2012). Utility of the P19 suppressor of gene-silencing protein for production of therapeutic antibodies in Nicotiana expression hosts. *Plant Biotechnology Journal, 10,* 1118–1128.

Gardner, A. M., Aviel, S., & Argon, Y. (1993). Rapid degradation of an unassembled immunoglobulin light chain is mediated by a serine protease and occurs in a pre-Golgi compartment. *Journal of Biological Chemistry, 268,* 25940–25947.

Gengenbach, B. B., Müschen, C. R., & Buyel, J. F. (2018). Expression and purification of human phosphatase and actin regulator 1 (PHACTR1) in plant-based systems. *Protein Expression and Purification, 151,* 46–55.

Hay, R. K. M. (1995). Harvest index: A review of its use in plant breeding and crop physiology. *Annals of Applied Biology, 126,* 197–216.

Hegde, R., Maiti, T. K., & Podder, S. K. (1991). Purification and characterization of three toxins and two agglutinins from *Abrus precatorius* seed by using lactamyl-Sepharose affinity chromatography. *Analytical Biochemistry, 194,* 101–109.

Hillmer, S., Movafeghi, A., Robinson, D. G., & Hinz, G. (2001). Vacuolar storage proteins are sorted in the cis-cisternae of the pea cotyledon Golgi apparatus. *Journal of Cell Biology, 152,* 41–50.

Holland, T., & Buyel, J. F. (2017). Bioreactor-based production of glycoproteins in plant cell suspension cultures. In Picanço e Castro, V., & Swiech, K. (Eds.), *Recombinant Glycoprotein Production* (pp. 129–146). New York: Springer.

Houdelet, M., Galinski, A., Holland, T., Wenzel, K., Schillberg, S., & Buyel, J. F. (2017). Animal component-free *Agrobacterium tumefaciens* cultivation media for better GMP-compliance increases biomass yield and pharmaceutical protein expression in *Nicotiana benthamiana*. *Biotechnology Journal, 12,* 1–10.

Howell, S., Kenmore, M., Kirkland, M., & Badley, R. A. (1998). High-density immobilization of an antibody fragment to a carboxymethylated dextran-linked biosensor surface. *Journal of Molecular Recognition, 11,* 200–203.

Jacobs, P. P., Geysens, S., Vervecken, W., Contreras, R., & Callewaert, N. (2009). Engineering complex-type N-glycosylation in *Pichia pastoris* using GlycoSwitch technology. *Nature Protocols, 4,* 58–70.

Jansing, J., & Buyel, J. F. (2018). The correlation between DsRed mRNA levels and transient DsRed protein expression in plants depends on leaf age and the 5′ untranslated region. *Biotechnology Journal, 14,* 1800075.

Jiang, Q. L., Zhang, S., Tian, M., Zhang, S. Y., Xie, T., Chen, D. Y., … Jiang, X. (2015). Plant lectins, from ancient sugar-binding proteins to emerging anti-cancer drugs in apoptosis and autophagy. *Cell Proliferation, 48,* 17–28.

Kastilan, R., Boes, A., Spiegel, H., Voepel, N., Chudobova, I., Hellwig, S., … Fischer, R. (2017). Improvement of a fermentation process for the production of two PfAMA1-DiCo-based malaria vaccine candidates in *Pichia pastoris*. *Scientific Reports, 7,* 11991.

Kim, S. H., Ryu, S. H., Lee, S. H., Lee, Y. H., Lee, S. R., Huh, J. W., … Chang, K. T. (2011). Instability of toxin A subunit of AB(5) toxins in the bacterial periplasm caused by deficiency of their cognate B subunits. *Biochimica et Biophysica Acta, 1808,* 2359–2365.

Kourmanova, A. G., Soudarkina, O. J., Olsnes, S., & Kozlov, J. V. (2004). Cloning and characterization of the genes encoding toxic lectins in mistletoe (*Viscum album* L). *European Journal of Biochemistry, 271,* 2350–2360.

Krauspenhaar, R., Rypniewski, W., Kalkura, N., Moore, K., DeLucas, L., Stoeva, S., … Betzel, C. (2002). Crystallisation under microgravity of mistletoe lectin I from *Viscum album* with adenine monophosphate and the crystal structure at 1.9 A resolution. *Acta Crystallographica, 58,* 1704–1707.

Lannoo, N., Vervecken, W., Proost, P., Rouge, P., & VanDamme, E. J. (2007). Expression of the nucleocytoplasmic tobacco lectin in the yeast *Pichia pastoris*. *Protein Expression and Purification, 53,* 275–282.

Lecoeur, J., & Sinclair, T. R. (2001). Harvest index increase during seed growth of field pea. *European Journal of Agronomy, 14,* 173–180.

Li, C. H., Narhi, L. O., Wen, J., Dimitrova, M., Wen, Z. Q., Li, J., … Jiang, Y. J. (2012). Effect of pH, temperature, and salt on the stability of *Escherichia coli*- and Chinese hamster ovary cell-derived IgG1 Fc. *Biochemistry, 51,* 10056–10065.

Lightfoot, E. N., Root, T. W., & O'Dell, J. L. (2008). Emergence of ideal membrane cascades for downstream processing. *Biotechnology Progress, 24,* 599–605.

Lindegaard, K. N., Adams, P. W., Holley, M., Lamley, A., Henriksson, A., Larsson, S., … Pisarek, M. (2016). Short rotation plantations policy history in Europe: Lessons from the past and recommendations for the future. *Food and Energy Security, 5,* 125–152.

Liu, H. F., Ma, J., Winter, C., & Bayer, R. (2010). Recovery and purification process development for monoclonal antibody production. *mAbs*, *2*, 480–499.

Lord, J. M. (1985). Precursors of ricin and *Ricinus communis* agglutinin. Glycosylation and processing during synthesis and intracellular transport. *European Journal of Biochemistry*, *146*, 411–416.

Ma, J. K., Drossard, J., Lewis, D., Altmann, F., Boyle, J., Christou, P., ... Fischer, R. (2015). Regulatory approval and a first-in-human phase I clinical trial of a monoclonal antibody produced in transgenic tobacco plants. *Plant Biotechnology Journal*, *13*, 1106–1120.

March, W. A., & Watson, D. M. (2007). Parasites boost productivity: Effects of mistletoe on litterfall dynamics in a temperate Australian forest. *Oecologia*, *154*, 339–347.

Merry, T., & Astrautsova, S. (2003). Chemical and enzymatic release of glycans from glycoproteins. *Methods in Molecular Biology*, *213*, 27–40.

Meshcheriakova, Y. A., Saxena, P., & Lomonossoff, G. P. (2014). Fine-tuning levels of heterologous gene expression in plants by orthogonal variation of the untranslated regions of a nonreplicating transient expression system. *Plant Biotechnology Journal*, *12*, 718–727.

Nandi, S., Kwong, A. T., Holtz, B. R., Erwin, R. L., Marcel, S., & McDonald, K. A. (2016). Techno-economic analysis of a transient plant-based platform for monoclonal antibody production. *mAbs*, *8*, 1–11.

Niwa, H., Tonevitsky, A. G., Agapov, I. I., Saward, S., Pfuller, U., & Palmer, R. A. (2003). Crystal structure at 3 A of mistletoe lectin I, a dimeric type-II ribosome-inactivating protein, complexed with galactose. *European Journal of Biochemistry*, *270*, 2739–2749.

Oliveira, C., Felix, W., Moreira, R. A., Teixeira, J. A., & Domingues, L. (2008). Expression of frutalin, an alpha-D-galactose-binding jacalin-related lectin, in the yeast Pichia pastoris. *Protein Expression and Purification*, *60*, 188–193.

Olsnes, S., Stirpe, F., Sandvig, K., & Pihl, A. (1982). Isolation and characterization of viscumin, a toxic lectin from *Viscum album* L. (mistletoe). *Journal of Biological Chemistry*, *257*, 13263–13270.

Opdensteinen, P., Clodt, J. I., Müschen, C. R., Filiz, V., & Buyel, J. F. (2018). A combined ultrafiltration/diafiltration step facilitates the purification of cyanovirin-N from transgenic tobacco extracts. *Journal of Biotechnology*, *6*, 206.

Pekarsky, A., Veiter, L., Rajamanickam, V., Herwig, C., Grunwald-Gruber, C., Altmann, F., & Spadiut, O. (2018). Production of a recombinant peroxidase in different glyco-engineered *Pichia pastoris* strains: A morphological and physiological comparison. *Microbial Cell Factories*, *17*, 183.

Piliarik, M., Vaisocherova, H., & Homola, J. (2009). Surface plasmon resonance biosensing. *Methods in Molecular Biology*, *503*, 65–88.

Purcell, O., Opdensteinen, P., Chen, W., Lowenhaupt, K., Brown, A., Hermann, M., ... Lu, T. K. (2017). Production of functional anti-Ebola antibodies in *Pichia pastoris*. *ACS Synthetic Biology*, *6*, 2183–2190.

Raab, D., Graf, M., Notka, F., Schodl, T., & Wagner, R. (2010). The GeneOptimizer Algorithm: Using a sliding window approach to cope with the vast sequence space in multiparameter DNA sequence optimization. *Systems and Synthetic Biology*, *4*, 215–225.

Richardson, P. T., Westby, M., Roberts, L. M., Gould, J. H., Colman, A., & Lord, J. M. (1989). Recombinant proricin binds galactose but does not depurinate 28 S ribosomal RNA. *FEBS Letters*, *255*, 15–20.

Severino, L. S., Auld, D. L., Baldanzi, M., Cândido, M. J. D., Chen, G., Crosby, W., ... Zieler, H. (2012). A review on the challenges for increased production of castor. *Agronomy Journal*, *104*, 853.

Simmons, B. M., & Russell, J. H. (1985). A single affinity column step method for the purification of ricin toxin from castor beans (*Ricinus communis*). *Analytical Biochemistry*, *146*, 206–210.

Simpson, J. C., Roberts, L. M., & Lord, J. M. (1996). Free ricin A chain reaches an early compartment of the secretory pathway before it enters the cytosol. *Experimental Cell Research*, *229*, 447–451.

Souza, M. A., Carvalho, F. C., Ruas, L. P., Ricci-Azevedo, R., & Roque-Barreira, M. C. (2013). The immunomodulatory effect of plant lectins: A review with emphasis on ArtinM properties. *Glycoconjugate Journal*, *30*, 641–657.

Spooner, R. A., Watson, P. D., Marsden, C. J., Smith, D. C., Moore, K. A., Cook, J. P., ... Roberts, L. M. (2004). Protein disulphide-isomerase reduces ricin to its A and B chains in the endoplasmic reticulum. *Biochemical Journal*, *383*, 285–293.

Stoger, E., Sack, M., Perrin, Y., Vaquero, C., Torres, E., Twyman, R. M., ... Fischer, R. (2002). Practical considerations for pharmaceutical antibody production in different crop systems. *Molecular Breeding*, *9*, 149–158.

Strasser, R. (2014). Biological significance of complex N-glycans in plants and their impact on plant physiology. *Frontiers of Plant Science*, *5*, 363.

Strasser, R. (2016). Plant protein glycosylation. *Glycobiology*, *26*, 926–939.

Sudhakar, A. (2009). History of cancer, ancient and modern treatment methods. *Journal of Cancer Science and Therapy*, *1*, 1–4.

Taubenschmid, J., Stadlmann, J., Jost, M., Klokk, T. I., Rillahan, C. D., Leibbrandt, A., ... Penninger, J. M. (2017). A vital sugar code for ricin toxicity. *Cell Research*, *27*, 1351–1364.

Tsuchiya, S., Yamabe, M., Yamaguchi, Y., Kobayashi, Y., Konno, T., & Tada, K. (1980). Establishment and characterization of a human acute monocytic leukemia cell line (THP-1). *International Journal of Cancer*, *26*, 171–176.

Uray, K., Mizuno, M., Inazu, T., Goto, K., & Hudecz, F. (2014). The effect of glycosylation on the antibody recognition of a MUC2 mucin epitope. *Biopolymers*, *102*, 390–395.

Urech, K., Schaller, G., & Jaggy, C. (2006). Viscotoxins, mistletoe lectins and their isoforms in mistletoe (*Viscum album* L.) extracts Iscador. *Arzneimittel-Forschung*, *56*, 428–434.

Walsh, M. J., Dodd, J. E., & Hautbergue, G. M. (2013). Ribosome-inactivating proteins: Potent poisons and molecular tools. *Virulence*, *4*, 774–784.

Walwyn, D. R., Huddy, S. M., & Rybicki, E. P. (2015). Techno-economic analysis of horseradish peroxidase production using a transient expression system in *Nicotiana benthamiana*. *Applied Biochemistry and Biotechnology*, *175*, 841–854.

Weidle, U. H., Schneider, B., Georges, G., & Brinkmann, U. (2012). Genetically engineered fusion proteins for treatment of cancer. *Cancer Genomics & Proteomics*, *9*, 357–372.

Wesche, J., Rapak, A., & Olsnes, S. (1999). Dependence of ricin toxicity on translocation of the toxin A-chain from the endoplasmic reticulum to the cytosol. *Journal of Biological Chemistry*, *274*, 34443–34449.

Zimran, A., Brill-Almon, E., Chertkoff, R., Petakov, M., Blanco-Favela, F., Munoz, E. T., ... Aviezer, D. (2011). Pivotal trial with plant cell-expressed recombinant glucocerebrosidase, taliglucerase alfa, a novel enzyme replacement therapy for Gaucher disease. *Blood*, *118*, 5767–5773.

Zwierzina, H., Bergmann, L., Fiebig, H., Aamdal, S., Schoffski, P., Witthohn, K., & Lentzen, H. (2011). The preclinical and clinical activity of aviscumine: A potential anticancer drug. *European Journal of Cancer*, *47*, 1450–1457

SUPPORTING INFORMATION

Additional supporting information may be found online in the Supporting Information section.